

# Amine Catalysis of $\beta$ -Ketol Dehydration. I. Catalysis by Aqueous Solutions of Tertiary Amines

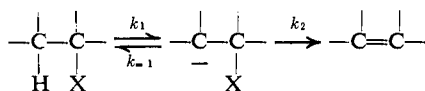
Donald J. Hupe, Martha C. R. Kendall, Gregory T. Sinner,  
and Thomas A. Spencer\*

Contribution from the Department of Chemistry, Dartmouth College,  
Hanover, New Hampshire 03755. Received August 2, 1972

**Abstract:** A kinetic study of the dehydration of 9-hydroxy-10-methyl-*cis*-decalone-2 (**1**) to form 10-methyl- $\Delta^{1,9}$ -octalone-2 (**2**) in aqueous solution has been made using hydroxide ion, hydronium ion, and a variety of tertiary amines as catalysts. Nonlinear dependence of  $k_{\text{obsd}}$  on catalyst concentration was found with hydroxide ion and unprotonated amines. For each catalyst a larger initial slope ( $k_{\text{B}}^i, k_{\text{OH}}^i$ ), proportional only to free base, was found at low catalyst concentrations, and a smaller final slope ( $k_{\text{B}}^f, k_{\text{OH}}^f$ ), also proportional to free base, was found at higher catalyst concentrations. The transition from initial to final slope occurred for all bases at  $k_{\text{C}}^f = 8.1 \times 10^{-7} \text{ sec}^{-1}$ . With lower  $\text{p}K_{\text{a}}$  tertiary amines, additional terms in the final slope proportional to protonated amine ( $k_{\text{A}}^f$ ) and hydronium ion ( $k_{\text{H}^+}^f$ ) were observed. With appropriately deuterated **1**, it was shown that exchange at the  $\alpha$  position involved in the dehydration occurred at high catalyst concentrations. These complex kinetic observations were analyzed in terms of a carbanionic elimination mechanism in which general base-catalyzed  $\alpha$ -proton abstraction is rate determining at low concentrations of hydroxide ion or tertiary amine, and breakdown of the enol **1e** or enolate anion **1<sup>-</sup>** derived from **1** is rate determining at high catalyst concentrations. The catalysis of the breakdown of intermediate enol and enolate anion has been analyzed quantitatively by assuming values of equilibrium concentrations of these species and a rapid equilibrium between them. Decisions between kinetically equivalent, plausible mechanistic possibilities for some of the kinetic terms arising from the conversion of intermediate (**1e**  $\rightleftharpoons$  **1<sup>-</sup>**) to **2** have been made with the aid of three-dimensional energy contour diagrams.

Mechanisms of  $\beta$ -elimination reactions have been extensively studied recently, particularly in cases where formation of an intermediate carbanion (Scheme I) is favored by its conjugation with a carbonyl<sup>1-6</sup> or

Scheme I



nitro<sup>7,8</sup> group, or because it is a 9-fluorenyl anion.<sup>9-11</sup> Molecules with a variety of leaving groups X<sup>-</sup> have been investigated, but the elimination of water from  $\beta$ -hydroxy ketones has not been thoroughly examined, despite the fact that such dehydrations are of considerable biochemical importance. There are enzymes which catalyze  $\beta$ -dehydration reactions *via* initial conversion of the carbonyl group to an iminium ion,<sup>12</sup> including 2-keto-3-deoxy-L-arabonate dehydratase,<sup>13</sup> 5-keto-4-deoxy-D-glucarate dehydratase,<sup>14</sup> and a pyrrole synthetase.<sup>15</sup> Other enzymes, such as  $\beta$ -hydroxydecanoyl thioester dehydrase<sup>16</sup> and those catalyzing dehydrations

in nucleotide-linked deoxy sugar synthesis,<sup>17</sup> apparently effect elimination of water without involvement of nucleophilic catalysis. Evidence has been obtained, for example, that the dehydration catalyzed by  $\beta$ -hydroxydecanoyl thioester dehydrase involves  $\alpha$ -proton abstraction from the substrate by a histidine imidazole moiety and general acid catalysis of the loss of hydroxide ion by a tyrosine phenol moiety.<sup>18</sup>

An important reason that detailed information on the catalysis of  $\beta$ -ketol dehydrations is lacking is that these substances usually have a complicating propensity to undergo reverse aldol reaction.<sup>19-23</sup> We report here an extensive study of the dehydration of 9-hydroxy-10-methyl-*cis*-decalone-2 (**1**), which proceeds quantitatively in aqueous solution to form the stable and chromophoric 10-methyl- $\Delta^{1,9}$ -octalone-2 (**2**). In this paper (part I) the catalysis of **1**  $\rightarrow$  **2** by aqueous solutions of tertiary amines is described, and in part II<sup>24</sup> the additional catalysis of this dehydration reaction *via* iminium ion formation by primary and secondary amines is considered.

## Results

$\beta$ -Hydroxy ketone **1** was readily prepared by the method of Marshall and Fanta.<sup>25</sup> The preparation of **1**-C<sub>1</sub>-d<sub>2</sub><sup>26</sup> involved Jones oxidation of the correspond-

(1) D. J. Hupe, M. C. R. Kendall, and T. A. Spencer, *J. Amer. Chem. Soc.*, **94**, 1254 (1972).

(2) L. R. Fedor, *ibid.*, **89**, 4479 (1967).

(3) L. R. Fedor, *ibid.*, **91**, 913 (1969).

(4) R. C. Cavestri and L. R. Fedor, *ibid.*, **92**, 4610 (1970).

(5) L. R. Fedor, *ibid.*, **91**, 908 (1969).

(6) L. R. Fedor and W. R. Glave, *ibid.*, **93**, 985 (1971).

(7) F. G. Bordwell, K. C. Yee, and A. C. Knipe, *ibid.*, **92**, 5945 (1970).

(8) F. G. Bordwell, M. M. Vestling, and K. C. Yee, *ibid.*, **92**, 5950 (1970).

(9) T. A. Spencer, M. C. R. Kendall, and I. D. Reingold, *ibid.*, **94**, 1250 (1972).

(10) R. A. More O'Ferrall and S. Slae, *J. Chem. Soc. B*, 260 (1970).

(11) R. A. More O'Ferrall, *ibid.*, 268 (1970).

(12) W. A. Wood, "The Enzymes," Vol. V, 3rd ed, P. D. Boyer, Ed., Academic Press, New York, N. Y., 1971, p 582.

(13) D. Portsmouth, A. C. Stoolmiller, and R. H. Abeles, *J. Biol. Chem.*, **242**, 2751 (1967).

(14) R. Jeffcoat, H. Hassall, and S. Dagley, *Biochem. J.*, 977 (1969).

(15) D. Shemin and D. L. Nandi, *Fed. Proc., Fed. Amer. Soc. Exp. Biol.*, **26**, 390 (1967).

(16) K. Bloch, in ref 12, p 441.

(17) L. Glaser and H. Zarkowsky in ref 12, p 465.

(18) G. M. Helmkamp, Jr., Doctoral Dissertation, Harvard University, 1970.

(19) F. H. Westheimer and H. Cohen, *J. Amer. Chem. Soc.*, **60**, 90 (1938).

(20) F. H. Westheimer, *Ann. N. Y. Acad. Sci.*, **39**, 401 (1940).

(21) D. S. Noyce and W. L. Reed, *J. Amer. Chem. Soc.*, **81**, 624 (1959).

(22) M. Stiles, D. Wolf, and G. V. Hudson, *ibid.*, **81**, 628 (1959).

(23) J. G. Miller and M. Kilpatrick, Jr., *ibid.*, **53**, 3217 (1931).

(24) D. J. Hupe, M. C. R. Kendall, and T. A. Spencer, *ibid.*, **95**, 2271 (1973).

(25) J. A. Marshall and W. I. Fanta, *J. Org. Chem.*, **29**, 2501 (1964).

(26) Compound **1**-C<sub>1</sub>-d<sub>2</sub> is actually 1,1,3,3,8,8-hexadeuterio-9-hydroxy-10-methyl-*cis*-decalone-2, as explained in the Experimental Section of ref 1.

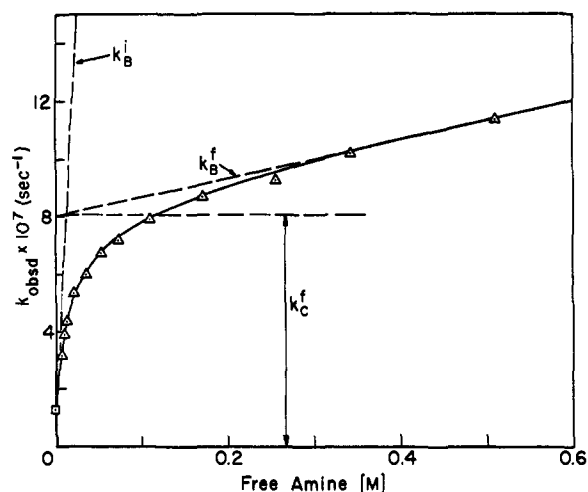
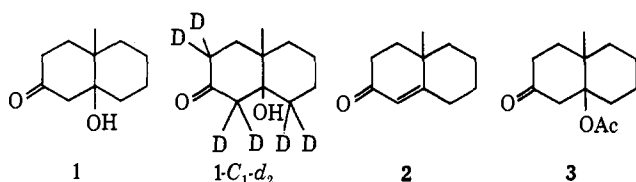


Figure 1. Plot of  $k_{\text{obsd}}$  values for the conversion of 1 to 2 vs. free imidazole concentration at pH 8.0. The initial slope ( $k_B^i$ ), final slope ( $k_B^f$ ), and the intercept of the final slope ( $k_C^f$ ) are indicated (---). The solid curve was computed using eq 3.

ingly labeled  $C_2$  alcohol, which was prepared as previously described.<sup>1</sup> This deuterated substrate was required in order to determine if the conversion of 1 to 2 would show a primary isotope effect.



The reactions of 1 and 1- $C_1$ - $d_2$  in dilute aqueous solution in the presence of tertiary amine buffers were monitored by observing the increase in absorbance at 247 nm caused by the formation of 2, in the same manner used to study the conversion of 3 to 2.<sup>1</sup> These reactions proceeded essentially quantitatively, giving no observable side products. Substrate 1 gave excellent pseudo-first-order kinetics under almost all catalytic circumstances.

The rate of formation of 2 from 1 showed a linear dependence on hydronium ion concentration:  $k_{\text{obsd}} = k_B^i[\text{H}_3\text{O}^+]$ , where  $k_B^i = 3.0 \times 10^{-6} \text{ M}^{-1} \text{ sec}^{-1}$  and  $[\text{H}_3\text{O}^+] = a_{\text{H}}$  as measured by pH meter. In contrast, nonlinear dependence of rate on catalyst concentration was found for hydroxide ion and amines. As a typical example of the change in slope encountered with increasing amine or hydroxide ion concentration, a plot of  $k_{\text{obsd}}$  vs. free amine concentration is shown in Figure 1 for imidazole at pH 8.0. The initial slope,  $k_B^i$ , at low catalyst concentrations changes to a lower slope,  $k_B^f$ , at higher catalyst concentrations. The  $k_{\text{obsd}}$  value at which the change in slope occurs (*i.e.*, the intercept of the final slope) is  $k_C^f = 8.1 \times 10^{-7}$ . The values of the constants  $k_B^i$  and  $k_B^f$ , corresponding to the initial and final slopes, were obtained at several pH's, as discussed below.

Figure 2 shows a log-log plot of the same data presented in Figure 1 and similar data for trimethylamine and hydroxide ion. In each case the larger initial slope  $k_B^i$  ( $k_{\text{OH}^-}$  for hydroxide ion) changes to a smaller final slope,  $k_B^f$  ( $k_{\text{OH}^-}$  for hydroxide ion), at the same  $k_C^f = 8.1 \times 10^{-7} \text{ sec}^{-1}$ , with both slopes being propor-

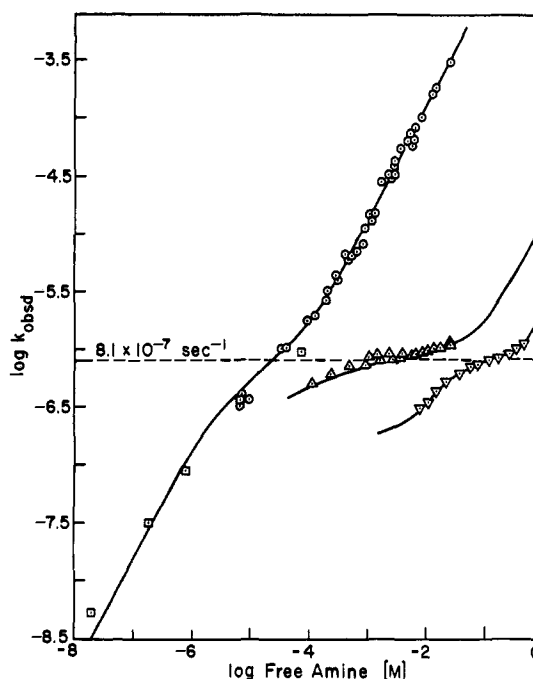


Figure 2. Plot of  $\log$  of  $k_{\text{obsd}}$  values for the conversion of 1 to 2 vs. the  $\log$  of the concentration of free base. Shown are the data obtained where the free base is hydroxide ion ( $\square$  or  $\circ$ ), the two symbols referring to points obtained by different experimental methods as described in the text), trimethylamine at pH 8.5 ( $\nabla$ ) and imidazole at pH 8.0 ( $\triangle$ ). All three catalysts exhibit a plateau (equivalent to a change in slope in a nonlogarithmic plot) at  $8.1 \times 10^{-7} \text{ sec}^{-1}$  (-----). The points are experimental and the solid lines were computed using eq 3 and the rate constants in Table I.

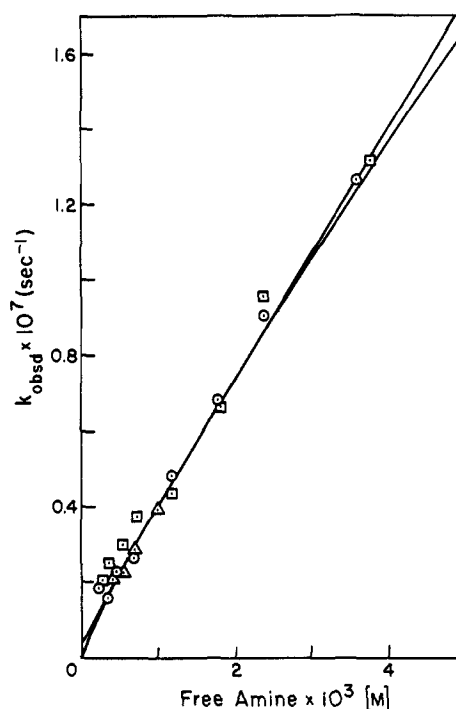


Figure 3. Plot of  $k_{\text{obsd}}$  values for the conversion of 1 to 2 vs. free amine concentration for *N*-methylimidazole at pH 6.2 ( $\square$ ), pH 5.5 ( $\circ$ ), and pH 5.0 ( $\triangle$ ). The solid lines were computed using eq 3. The computed lines for pH 5.0 and 5.5 coincide.

tional to free base concentration. The values of  $k_B^i$  listed in Table I were obtained at low pH to avoid interference from hydroxide ion catalysis. As shown in Figure 3, using *N*-methylimidazole, the initial slope

Table I. Rate Constants for the Reaction of 1 to Form 2 in Aqueous Solution at 25°

Catalyst	$pK_a^a$	Initial slopes, $M^{-1} \text{sec}^{-1}$	Final slopes, $M^{-1} \text{sec}^{-1}$	No. of runs
Hydronium ion		$k_{H^+}^i = 3.0 \times 10^{-5}$	$k_{H^+}^f = 2.0 \times 10^6$	10
Hydroxide ion	15.7	$k_{OH^-}^i = 1.56 \times 10^{-1}$	$k_{OH^-}^f = 1.31 \times 10^{-2}$	39
Quinuclidine	10.95	$k_B^i = 4.8 \times 10^{-2}$	$k_B^f = 7.2 \times 10^{-5}$	80
Triethylamine	10.75	$k_B^i = 4 \times 10^{-3}$	$k_B^f = 2 \times 10^{-5}$	24
Trimethylamine	9.76	$k_B^i = 4 \times 10^{-3}$	$k_B^f = 1.1 \times 10^{-5}$	104
Diazabicyclo[2.2.2]octane	8.70	$k_B^i = 2.4 \times 10^{-3}$	$k_B^f = 5.4 \times 10^{-6}$	12
<i>N</i> -Methylmorpholine	7.41	$k_B^i = 7 \times 10^{-5}$	$k_B^f = 1.8 \times 10^{-7}$ ; $k_A^f = 1.5 \times 10^{-6}$	60
<i>N</i> -Methylimidazole	7.06	$k_B^i = 3.6 \times 10^{-5}$	$k_B^f = 2.3 \times 10^{-7}$ ; $k_A^f = 2 \times 10^{-6}$	84
Imidazole	6.95	$k_B^i = 5.1 \times 10^{-5}$	$k_B^f = 6.7 \times 10^{-7}$ ; $k_A^f = 5.8 \times 10^{-7}$	92
Dimethylcyanomethylamine	4.20	$k_B^i = 5.1 \times 10^{-6}$	$c$	32
Constant term			$k_C^f = 8.1 \times 10^{-7} \text{sec}^{-1}$	

<sup>a</sup> The sources of all the  $pK_a$  values are given in ref 2. <sup>b</sup> Determined indirectly; no change in slope observed. <sup>c</sup> Not measurable; see text.

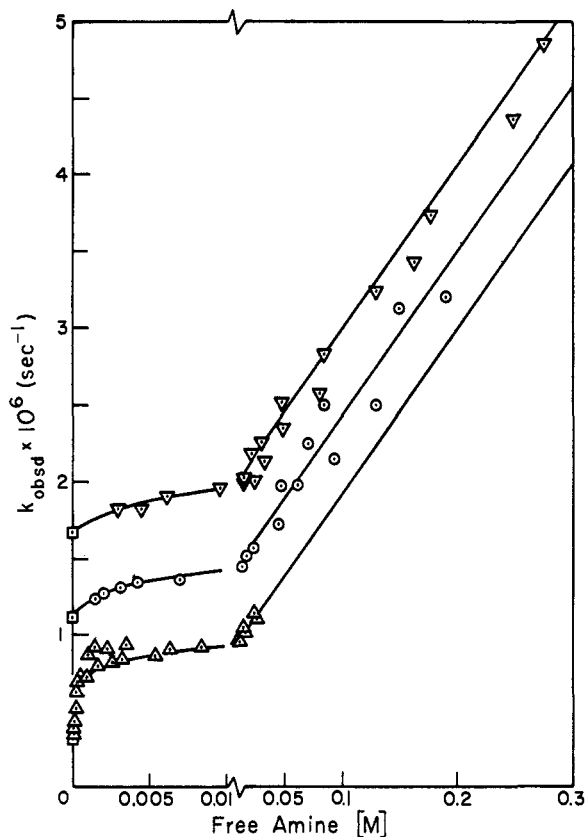


Figure 4. Plot of  $k_{\text{obsd}}$  values for the conversion of 1 to 2 vs. free trimethylamine concentration at pH 9.9 ( $\nabla$ ), pH 9.6 ( $\circ$ ), and pH 8.5 ( $\Delta$ ). The solid lines were computed using eq 3, as were the intercepts ( $\square$ ) which reflect hydroxide ion catalysis.

obtained by plotting  $k_{\text{obsd}}$  vs. free amine concentration is invariant with a change in pH, indicating the absence of a significant term proportional to protonated amine concentration.

The final slopes proportional to free amine concentration ( $k_B^f$ ) were usually measured at pH's above the amine  $pK_a$  so that high concentrations of free amine could be attained. For amines with  $pK_a > 8$  the final slopes of plots of  $k_{\text{obsd}}$  vs. [free amine] were invariant with changing pH, as illustrated in Figure 4 for trimethylamine. For lower  $pK_a$  tertiary amines, the situation was more complicated, as discussed below. Values of  $k_B^f$  are also listed in Table I.

The pattern of large initial slope changing to the smaller final slope at  $8.1 \times 10^{-7} \text{sec}^{-1}$  is present for all of the amines at pH's near neutrality, but at higher

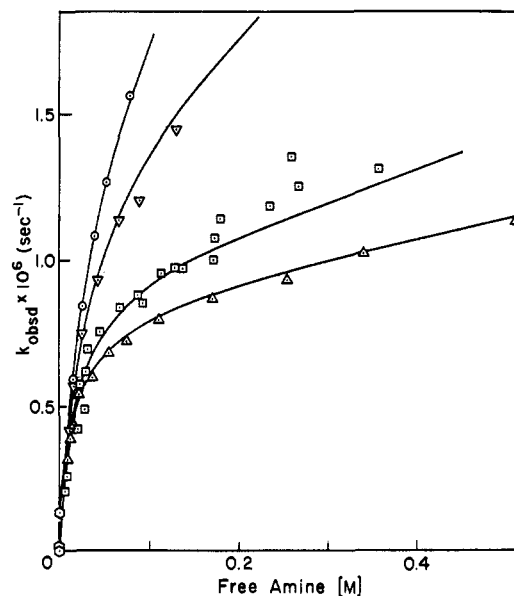


Figure 5. Plot of  $k_{\text{obsd}}$  values for the conversion of 1 to 2 vs. free imidazole concentration at pH 6.14 ( $\circ$ ), pH 6.40 ( $\nabla$ ), pH 7.05 ( $\square$ ), and pH 8.0 ( $\Delta$ ). The solid lines and the intercepts ( $\circ$ ) were computed using eq 3.

hydroxide ion concentrations only the final slope is observed, with the intercept being equal to the hydroxide ion catalysis at that pH. Such extrapolation to zero buffer concentration was not generally useful for determining data on hydroxide ion catalysis, however, due to the change in slope which occurs at very low buffer concentrations in most cases. Hydroxide ion catalysis was therefore studied in the absence of buffer. The values of  $k_{\text{obsd}}$  obtained for unbuffered solutions at pH  $> 10$  were plotted vs. hydroxide ion concentration to yield  $k_{OH^-}^f$ . The values of  $k_{\text{obsd}}$  obtained at pH  $< 9$  were plotted vs. hydroxide ion concentration to obtain  $k_{OH^-}^i$ , and these constants are listed in Table I. Special procedures were required to measure  $k_{\text{obsd}}$  values at pH's near neutrality for these unbuffered runs. Because these reactions were very slow, it was necessary to use high concentrations of 1 and a long path length cell, and to observe only a very small fraction of the reaction. It was also necessary to protect the reaction mixture against  $CO_2$  absorption. The points obtained in this manner are marked with squares in Figure 2.

Three of the amines with  $pK_a \approx 7$ , imidazole, *N*-methylimidazole, and *N*-methylmorpholine, diverged

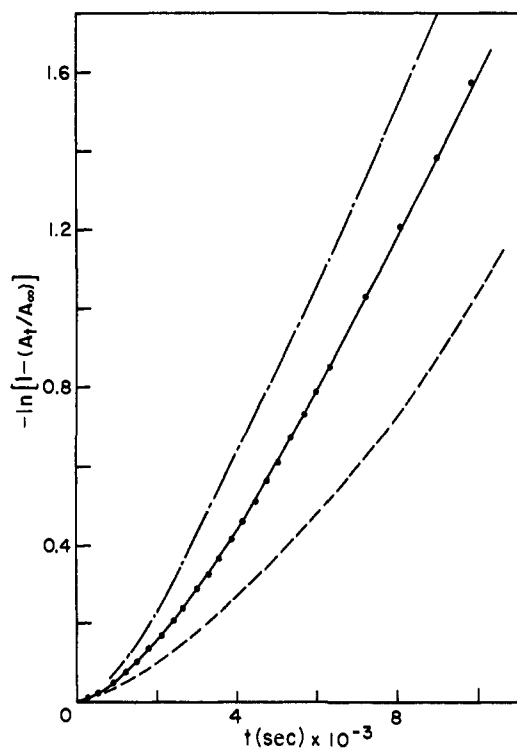


Figure 6. Pseudo-first-order plot of  $-\ln(1 - (A_t/A_\infty))$  vs.  $t$  (sec) obtained for the conversion of 1- $C_1$ - $d_2$  to 2 at pH 12.40 in the absence of buffer. The points are experimental and the lines were computed using the method described in the text and eq 4 for  $k_{-1}/k_2 = 25$  (---),  $k_{-1}/k_2 = 5$  (-·-·-), and  $k_{-1}/k_2 = 12$  (—).

from the pattern outlined above. In addition to the final slope term proportional to free amine (measured at pH's well above the  $pK_a$ ), these amines yielded final slope terms proportional to protonated amine concentration ( $k_A^f$ ) and hydronium ion concentration ( $k_H^f$ ). As shown in Figure 5, with imidazole as the catalyst, the final slope increases as the pH is decreased owing to the presence of the  $k_A^f[R_3NH^+]$  term, and the  $k_{obsd}$  value at which the change from the initial  $k_B^f$  slope occurs increases with decreasing pH owing to the  $k_H^f[H_3O^+]$  term.

Data for these  $k_A^f$  and  $k_H^f$  terms were relatively difficult to obtain because the final slopes can only be observed at high concentrations of free amine. With high- $pK_a$  amines, which have relatively large  $k_B^f$  terms and relatively small  $k_A^f$  terms, the latter could not be detected. Final slope terms for a fourth low- $pK_a$  amine, dimethylcyanomethylamine, could not be measured because the catalyst decomposed too rapidly under conditions appropriate for determination of  $k_A^f$ . The value of  $k_H^f$  and the values of  $k_A^f$  for imidazole, *N*-methylimidazole, and *N*-methylmorpholine listed in Table I are those which give the best fit with experimental data, but they are somewhat uncertain because of the experimental limitations outlined above.

The dehydration of 1- $C_1$ - $d_2$  exhibited a primary kinetic isotope effect with both amines and hydroxide ion. In Figures 6 and 7 are shown plots of  $\ln(1/(1 - A_t/A_\infty))$  vs. time for 1- $C_1$ - $d_2$  with hydroxide ion and trimethylamine, respectively. Such plots with 1 as substrate are straight lines with slope =  $k_{obsd}$ , but with 1- $C_1$ - $d_2$  they are curved, showing a large initial isotope effect which diminishes as the reaction progresses.

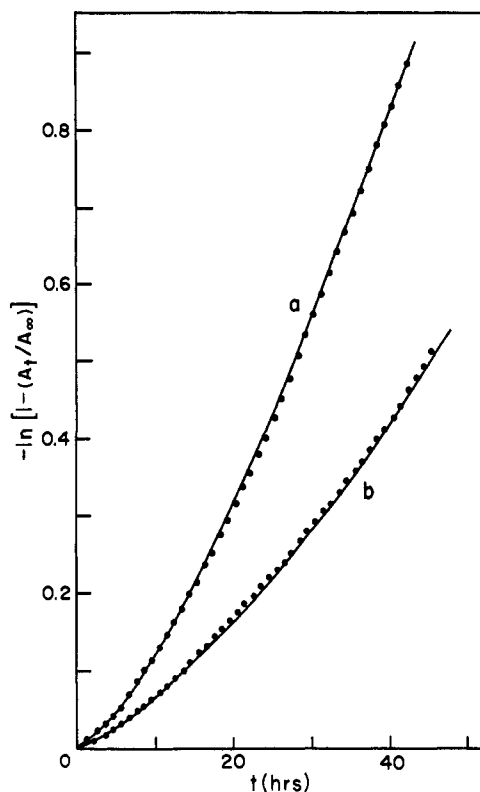


Figure 7. Pseudo-first-order plot of  $-\ln(1 - (A_t/A_\infty))$  for the conversion of 1- $C_1$ - $d_2$  to 2 vs.  $t$  (hr) at pH 8.50 with (a) 0.44 *M* and (b) 0.15 *M* total trimethylamine buffer concentrations. The points are experimental and the lines were computed using eq 4 for (a)  $k_{-1}/k_2 = 90$  and (b)  $k_{-1}/k_2 = 37$ .

The slope eventually approximates that for 1 under the same reaction conditions.

## Discussion

The kinetic behavior of elimination reactions of the type shown in Scheme I depends on the nature of the leaving group  $X^-$ . When  $X^-$  is a good leaving group like acetate ion,<sup>1,2,3,7</sup> benzoate ion,<sup>4</sup> or chloride ion,<sup>9</sup> general base catalysis has been observed and mechanisms involving rate-determining  $\alpha$ -proton abstraction have been postulated ( $k_2 > k_{-1}$ ). When  $X^-$  is a poorer leaving group like hydroxide ion<sup>7,8</sup> or methoxide ion,<sup>5,7,8</sup> specific base catalysis has been observed, and rate-determining breakdown of an equilibrium concentration of carbanion to form product has been proposed ( $k_{-1} > k_2$ ).

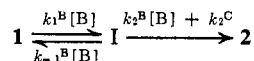
Fedor's study<sup>6</sup> of the elimination reaction of  $\beta$ -phenoxy ketones, where the leaving group ability is intermediate between the types discussed above, provides the closest parallel in kinetic behavior with the present study. First-order dependence on general base at low catalyst concentration, changing to zero-order dependence on general base at higher catalyst concentrations, was observed.<sup>6</sup> In the absence of complex formation, such a downward-curving slope with increasing catalyst concentration is indicative of a change in rate-determining step, and, therefore, of the existence of an intermediate.<sup>27</sup> For the  $\beta$ -phenoxy ketone elimination reaction, this behavior was inter-

(27) W. P. Jencks, "Catalysis in Chemistry and Enzymology," McGraw-Hill, New York, N. Y., 1969.

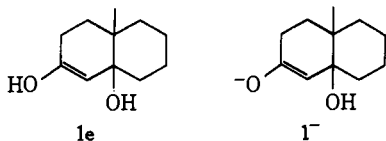
preted as indicating a change from a situation where  $k_2 > k_{-1}$  to one where  $k_{-1} > k_2$  in Scheme I.

The data for the dehydration of **1** can be explained by a fundamentally similar, but substantially more complicated, mechanistic proposal. Considering the rate data in Figure 1, and ignoring hydroxide ion catalysis for the moment, a proposed mechanism must predict that  $d[2]/dt = k_B^i[B][1]$  at low values of  $[B]$  and that  $d[2]/dt = (k_B^f[B] + k_C^f)[1]$  at high  $[B]$ . The mechanism in Scheme II satisfies these conditions if  $(k_2^B[B] + k_2^C) > (k_{-1}^B[B])$  at low  $[B]$  and  $(k_{-1}^B[B]) > (k_2^B[B] + k_2^C)$  at high  $[B]$ . As discussed below, in order to account most reasonably for all of the observed kinetic terms it is necessary to postulate that the intermediate species in the dehydration can be either the enol **1e** or the enolate anion **1<sup>-</sup>**, although Scheme II as written requires that **I** = **1e**.

#### Scheme II



+  $k_2^C) > (k_{-1}^B[B])$  at low  $[B]$  and  $(k_{-1}^B[B]) > (k_2^B[B] + k_2^C)$  at high  $[B]$ . As discussed below, in order to account most reasonably for all of the observed kinetic terms it is necessary to postulate that the intermediate species in the dehydration can be either the enol **1e** or the enolate anion **1<sup>-</sup>**, although Scheme II as written requires that **I** = **1e**.



A steady state assumption on **I** in Scheme II yields eq 1. At low values of  $[B]$ ,  $d[2]/dt = k_1^B[B][1]$ , con-

$$d[2]/dt = k_1^B[B] \frac{k_2^B[B] + k_2^C}{k_{-1}^B[B] + k_2^B[B] + k_2^C} [1] \quad (1)$$

sistent with observed data when  $k_1^B = k_B^i$ . If, at high concentrations of  $[B]$ ,  $k_{-1}^B[B] \gg (k_2^B[B] + k_2^C)$ , then an equilibrium concentration of **I** will exist where  $K = [I]/[1] = k_1^B/k_{-1}^B$ . Under such conditions  $d[2]/dt = K(k_2^B[B] + k_2^C)[1]$ , which is consistent with observed data when  $Kk_2^B = k_B^f$  and  $Kk_2^C = k_C^f$ . By multiplying the numerator and denominator in eq 1 by  $K$ , and by using the equalities above,  $d[2]/dt$  may be expressed entirely in terms of the measured  $k_B^i$ ,  $k_B^f$ , and  $k_C^f$  values listed in Table I, as shown in eq 2.

$$d[2]/dt = k_B^i[B] \frac{k_B^f[B] + k_C^f}{k_B^i[B] + k_B^f[B] + k_C^f} [1] \quad (2)$$

While the data obtained are consistent with Scheme II, no specific mechanisms are implied at this point for the individual terms. For example, if **I** can be either **1e** or **1<sup>-</sup>**, then  $k_B^i[B]$  may be due to any reaction of **1e** with **B** or any reaction of **1<sup>-</sup>** with  $BH^+$ , because these would be kinetically equivalent. Individual mechanistic details of this type are considered later.

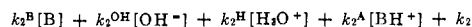
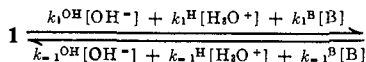
The same procedures employed with Scheme II can be used to formulate the mechanism in Scheme III, which yields the general rate expression for the formation of **2** from **1** given in eq 3. As in eq 2,  $d[2]/dt$  is

$$\frac{d[2]}{dt} = (k_B^i[B] + k_{OH}^i[OH^-] + k_H^i[H_3O^+]) \times$$

$$\left[ \frac{k_B^f[B] + k_{OH}^f[OH^-] + k_A^f[BH^+] + k_H^f[H_3O^+] + k_C^f}{k_B^i[B] + k_{OH}^i[OH^-] + k_H^i[H_3O^+] + k_B^f[B] + k_{OH}^f[OH^-] + k_A^f[BH^+] + k_H^f[H_3O^+] + k_C^f} \right] [1] \quad (3)$$

expressed entirely in terms of the measured initial slopes ( $k_{OH}^i$ ,  $k_B^i$ ,  $k_H^i$ ) and the measured final slopes ( $k_{OH}^f$ ,  $k_B^f$ ,  $k_A^f$ ,  $k_H^f$ ,  $k_C^f$ ). When the observed slopes

#### Scheme III



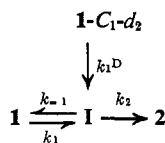
listed in Table I are used in eq 3, it accurately predicts the  $k_{obsd}$  values measured for all of the catalysts studied, as indicated by the fit of measured with computed rates in Figures 1-5. Equation 3 also predicts the absence of initial slope at high pH's indicated in Figure 4 for trimethylamine. At high pH's the equilibrium between **1** and **I** is established by hydroxide ion alone ( $k_{-1} > k_2$ ), and an initial slope caused by free amine (which requires  $k_2 > k_{-1}$ ) cannot be observed under such conditions.

If the values of the initial slopes  $k_{OH}^i$  and  $k_B^i$  represent rate-determining formation of **I**, they are rate constants for general base-catalyzed  $\alpha$ -proton abstraction from **1** to form **1<sup>-</sup>**. As such, they should form a Brønsted plot similar to the one obtained for the same amines with keto acetate **3**, in which  $\alpha$ -proton abstraction is known to be rate determining.<sup>1</sup> In Figure 8 the values of  $\log k_B^i$  and  $\log k_{OH}^i$  and the rate constants for general base-catalyzed  $\alpha$ -proton abstraction ( $k_B$ ) from **3** with the same amines are plotted against the amine  $pK_a$ 's. Both the Brønsted  $\beta$ 's and the absolute values of the constants are similar. The fact that  $k_B^i$  and  $k_{OH}^i$  values for **1** are slightly smaller than the corresponding  $k_B$  and  $k_{OH}$  values for **3** is consistent with Fedor's finding of a very small increase in  $\alpha$ -proton abstraction rate with increasing leaving group ability for 4-(4-substituted-benzoyloxy)-2-butanones.<sup>4</sup>

A prediction demanded by the proposed mechanism in Scheme III is that there will be no  $\alpha$ -proton exchange under catalytic conditions producing a point on the initial slope, where  $k_2 > k_{-1}$ . For a point on the final slope, however,  $k_{-1} > k_2$  and exchange should occur. This has been tested quantitatively by comparing the ratio  $k_{-1}/k_2$  measured in exchange experiments on **1-C<sub>1</sub>-d<sub>2</sub>** with the ratio calculated for the mechanism in Scheme III from the constants in Table I. Figure 6 shows the pseudo-first-order plot obtained for the formation of **2** from **1-C<sub>1</sub>-d<sub>2</sub>** at pH 12.40 with no amine catalyst. Such a plot for substrate **1** yields a straight line with a slope equal to  $k_{obsd}$  for those conditions. With **1-C<sub>1</sub>-d<sub>2</sub>**, however, the slope at the beginning of the reaction ( $k_{obsd}^{t=0}$ ) was about one-sixth the value observed for **1** under the same conditions. As the reaction progressed, the slope increased to a final value ( $k_{obsd}^{t=\infty}$ ) that was close to the  $k_{obsd}$  value for **1** under the same conditions. This increase in  $k_{obsd}$ , reflecting a diminution of the primary kinetic isotope effect, occurs because **1-C<sub>1</sub>-d<sub>2</sub>** becomes protonated at  $C_1$  through isotopic exchange *via* **I** (Scheme IV). Similar behavior was observed in the dehydration of deu-

terated 9-fluorenylmethanol.<sup>10</sup> It is not known whether the exchange of H for D at  $C_1$  involves one or two of the deuterium atoms at that site; therefore, species **1**,

Scheme IV



1, and 2 in Scheme IV and the related discussion may contain either one or no deuterons at  $C_1$ .

When  $k_{-1}/k_2$  is large, exchange is rapid and only a small fraction of a half-life is needed to protonate  $1-C_1-d_2$ . Many half-lives are required if the ratio  $k_{-1}/k_2$  is small. Thus, in principle there is a method for determining  $k_{-1}/k_2$  under any given catalytic circumstances. In order to obtain values of  $k_{-1}/k_2$  it is necessary to use the integrated rate equation for the process outlined in Scheme IV with experimental values inserted for  $k_{\text{obsd}}^{t=0}$  and  $k_{\text{obsd}}^{t=\infty}$ , varying  $k_{-1}/k_2$  until the best fit is obtained.

If it is assumed that no elimination reaction occurs without the intermediacy of I, and if a steady state assumption is made on [I], then

$$d[2]/dt = k_2[I] = \frac{k_1^D k_2}{k_{-1} + k_2} [1-C_1-d_2] + \frac{k_1 k_2}{k_{-1} + k_2} [1]$$

where  $k_1^D$  is the rate constant for the conversion of  $1-C_1-d_2$  to I. More O'Ferrall<sup>10</sup> has solved a closely analogous kinetic problem by integration of an almost identical equation. In the same manner, the present expression may be put into a form suitable for integration by utilizing the stoichiometric relationships among [1],  $[1-C_1-d_2]$ , and [2]. After integration, algebraic manipulation can be used to obtain eq 4 which is of

$$\begin{aligned}
 -\ln\left(1 - \frac{[2]_t}{[2]_{t=\infty}}\right) &= -\ln\left\{\left(\frac{1 - (k_1^D/k_1)}{1 - \left(\frac{k_1^D}{k_1}\right)\left(\frac{k_{-1} + k_2}{k_2}\right)}\right) \times \right. \\
 &[\exp(-k_1^D t)] + \left. \left(1 - \frac{1 - (k_1^D/k_1)}{1 - \left(\frac{k_1^D}{k_1}\right)\left(\frac{k_{-1} + k_2}{k_2}\right)}\right) \times \right. \\
 &\left. \exp\left(-\frac{k_1 k_2 t}{k_{-1} + k_2}\right)\right\} \quad (4)
 \end{aligned}$$

the form  $-\ln(1 - ([2]_t/[2]_{\infty})) = f(t)$ .<sup>28</sup> The equivalent function  $-\ln(1 - A_t/A_{\infty})$  can be plotted vs. time to obtain pseudo-first-order plots such as the one in Figure 6. The initial  $k_{\text{obsd}}$  value,  $k_{\text{obsd}}^{t=0}$ , which embodies the kinetic isotope effect, can be measured and set equal to  $k_1^D k_2 / (k_{-1} + k_2)$ , since this is the rate at which I is formed from  $1-C_1-d_2$ , times the fraction of I which goes to product. Similarly, the measured final  $k_{\text{obsd}}$  value,  $k_{\text{obsd}}^{t=\infty}$ , is equal to  $k_1 k_2 / (k_{-1} + k_2)$ . Thus  $k_1^D = (k_{\text{obsd}}^{t=0}) / (k_2 / (k_{-1} + k_2))$  and  $k_1 = (k_{\text{obsd}}^{t=\infty}) / (k_2 / (k_{-1} + k_2))$ . If a ratio of  $k_{-1}$  to  $k_2$  is chosen, the function of  $t$  in eq 4 becomes completely defined, and if this ratio is varied a series of computed curves like those in Figure 6 can be obtained.

The best fit with the experimental data for the hydroxide ion catalyzed runs at pH 12.40 was found when  $k_{-1}/k_2 = 12$ . This ratio may be compared with that predicted by Scheme III and the observed values of  $k_{\text{OH}^+}[\text{OH}^-]$ ,  $k_{\text{OH}^+}[\text{OH}^-]$ , and  $k_{\text{C}^+}$  under the same condi-

(28) For details, see D. J. Hupe, Ph.D. Thesis, Dartmouth College, 1972.

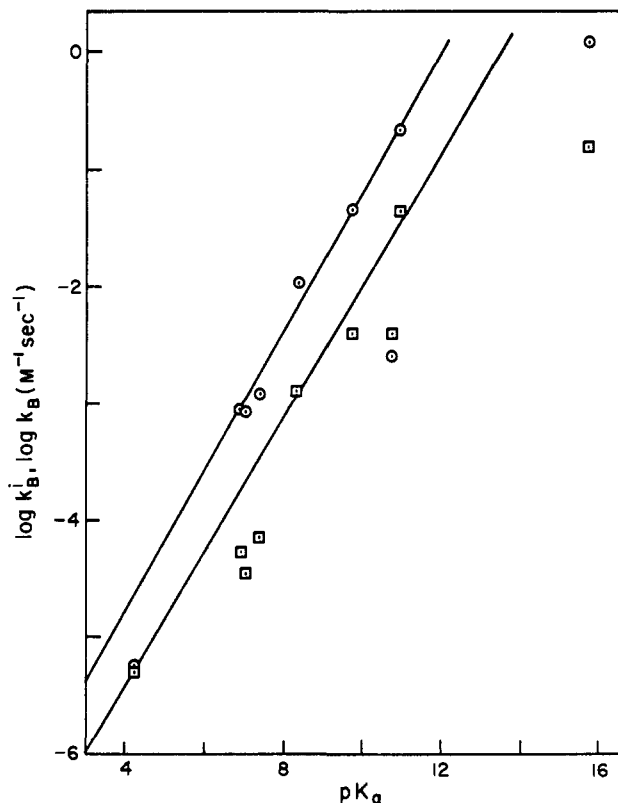


Figure 8. Brønsted plots of  $\log k_B^D$  values from Table I (□) vs. tertiary amine  $pK_a$ 's, and of  $\log k_B$  values from ref 1 (○) vs. the same amine  $pK_a$ 's. The slopes are  $\beta = 0.59$ . The points for the diamine diazabicyclo[2.2.2]octane have been corrected according to the equation given by Jencks, ref 27, p 173.

tions. With hydroxide ion as the sole catalyst,  $k_{\text{OH}^+}[\text{OH}^-] = k_1$ , and  $k_{\text{OH}^+}[\text{OH}^-] + k_{\text{C}^+} = k_1[k_2 / (k_{-1} + k_2)]$ , so that

$$\frac{k_{\text{OH}^+}[\text{OH}^-]}{k_{\text{OH}^+}[\text{OH}^-] + k_{\text{C}^+}} = \frac{k_1}{k_1[k_2 / (k_{-1} + k_2)]} = \frac{k_{-1} + k_2}{k_2} = \frac{k_{-1}}{k_2} + 1$$

Thus  $k_{-1}/k_2 = \{k_{\text{OH}^+}[\text{OH}^-] / (k_{\text{OH}^+}[\text{OH}^-] + k_{\text{C}^+})\} - 1$ . At pH 12.40 this predicts that  $k_{-1}/k_2 = \{(0.156 \times 2.5 \times 10^{-2}) / [(1.31 \times 10^{-2} \times 2.5 \times 10^{-2}) + (8.1 \times 10^{-7})]\} - 1 = 11.9 - 1 = 10.9$ , in good agreement with the value of 12 measured in the exchange experiment.

By the same means, the values of  $k_{-1}/k_2$  obtained in exchange experiments with trimethylamine at pH 8.50 with 0.44 and 0.15 M total amine concentrations may be compared with the computed values. The best fits in Figure 7 were obtained with  $k_{-1}/k_2 = 90$  and 37, respectively, for the two amine concentrations. The corresponding values computed from the constants in Table I using  $k_{-1}/k_2 = [(k_{\text{OH}^+}[\text{OH}^-] + k_b^+[\text{R}_3\text{N}]) / (k_{\text{OH}^+}[\text{OH}^-] + k_b^+[\text{R}_3\text{N}] + k_H^+[\text{H}^+] + k_{\text{C}^+})] - 1$  are 83 and 31, again in good agreement with the exchange experimental values. The evidence is excellent then that the mechanism of dehydration of 1 involves rate-determining general base-catalyzed  $\alpha$ -proton abstraction at low concentrations of hydroxide ion and free amine, accounting for the large initial slopes, while at high concentrations the breakdown of an equilibrium concentration of intermediate to product is the slow step.

Both keto acetate 3 and ketol 1 exhibit terms in their

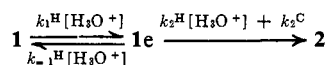
Table II. Rate Constants for the Reactions of 1, 1<sup>-</sup> to 1e with General Acids and Bases in Aqueous Solution at 25°

Catalyst	pK <sub>a</sub> <sup>a</sup>	k <sub>1</sub> , M <sup>-1</sup> sec <sup>-1</sup>	k <sub>-1</sub> , M <sup>-1</sup> sec <sup>-1</sup>	k <sub>2</sub> , M <sup>-1</sup> sec <sup>-1</sup>	k <sub>3</sub> , M <sup>-1</sup> sec <sup>-1</sup>
Hydronium ion		k <sub>1</sub> <sup>H</sup> = 3.0 × 10 <sup>-5</sup>	k <sub>-1</sub> <sup>H</sup> = 7.3 × 10 <sup>0</sup>	k <sub>2</sub> <sup>H</sup> = 4.05 × 10 <sup>10</sup>	k <sub>3</sub> <sup>H</sup> = 4.8 × 10 <sup>6</sup>
Hydroxide ion	15.7	k <sub>1</sub> <sup>OH</sup> = 1.56 × 10 <sup>-1</sup>	k <sub>-1</sub> <sup>H<sub>2</sub>O</sup> = 1.42 × 10 <sup>0</sup> b		
Quinuclidine	10.95	k <sub>1</sub> <sup>B</sup> = 4.5 × 10 <sup>-2</sup>	k <sub>-1</sub> <sup>A</sup> = 2.5 × 10 <sup>4</sup>	k <sub>2</sub> <sup>A</sup> = 4.0 × 10 <sup>1</sup>	
Triethylamine	10.75	k <sub>1</sub> <sup>B</sup> = 4 × 10 <sup>-3</sup>	k <sub>-1</sub> <sup>A</sup> = 3.5 × 10 <sup>3</sup>	k <sub>2</sub> <sup>A</sup> = 1.8 × 10 <sup>1</sup>	
Trimethylamine	9.76	k <sub>1</sub> <sup>B</sup> = 4 × 10 <sup>-3</sup>	k <sub>-1</sub> <sup>A</sup> = 3.5 × 10 <sup>4</sup>	k <sub>2</sub> <sup>A</sup> = 9.4 × 10 <sup>1</sup>	
Diazabicyclo[2.2.2]octane	8.70	k <sub>1</sub> <sup>B</sup> = 2.5 × 10 <sup>-3</sup>	k <sub>-1</sub> <sup>A</sup> = 2.5 × 10 <sup>5</sup>	k <sub>2</sub> <sup>A</sup> = 5.4 × 10 <sup>2</sup>	
N-Methylmorpholine	7.41	k <sub>1</sub> <sup>B</sup> = 7 × 10 <sup>-5</sup>	k <sub>-1</sub> <sup>A</sup> = 1.4 × 10 <sup>5</sup>	k <sub>2</sub> <sup>A</sup> = 3.4 × 10 <sup>2</sup>	k <sub>3</sub> <sup>A</sup> = 3.6 × 10 <sup>-1</sup>
N-Methylimidazole	7.06	k <sub>1</sub> <sup>B</sup> = 3.6 × 10 <sup>-5</sup>	k <sub>-1</sub> <sup>A</sup> = 1.6 × 10 <sup>5</sup>	k <sub>2</sub> <sup>A</sup> = 1.0 × 10 <sup>3</sup>	k <sub>3</sub> <sup>A</sup> = 5 × 10 <sup>-1</sup>
Imidazole	6.95	k <sub>1</sub> <sup>B</sup> = 5.05 × 10 <sup>-5</sup>	k <sub>-1</sub> <sup>A</sup> = 2.8 × 10 <sup>5</sup>	k <sub>2</sub> <sup>A</sup> = 3.7 × 10 <sup>3</sup>	k <sub>3</sub> <sup>A</sup> = 1.4 × 10 <sup>-1</sup>
Dimethylcyanomethylamine	4.20	k <sub>1</sub> <sup>B</sup> = 5.1 × 10 <sup>-6</sup>	k <sub>-1</sub> <sup>A</sup> = 1.6 × 10 <sup>7</sup>		
Water	-1.7			k <sub>2</sub> <sup>H<sub>2</sub>O</sup> = 1.42 × 10 <sup>-1</sup> b,c	

<sup>a</sup> The sources of all the pK<sub>a</sub> values are given in ref 2. <sup>b</sup> Calculation of these rate constants involved division by 55 M to account for [H<sub>2</sub>O]. <sup>c</sup> Equivalent to the first-order rate constant for 1<sup>-</sup> → 2 = k<sub>2</sub><sup>C</sup> = 7.83 × 10<sup>1</sup> sec<sup>-1</sup> (see text).

rate expressions proportional to hydronium ion concentration, with rate constants k<sub>H</sub> = 8.0 × 10<sup>-5</sup> M<sup>-1</sup> sec<sup>-1</sup> and k<sub>H</sub><sup>i</sup> = 3.0 × 10<sup>-5</sup> M<sup>-1</sup> sec<sup>-1</sup>, respectively. The similarity in magnitude of these rate constants suggests that hydronium ion catalyzed enolization, which does not involve the differing leaving groups, is rate determining. Unlike the other catalysts discussed above, hydronium ion does *not* exhibit a change in slope with increasing catalyst concentration. The mechanism proposed in Scheme V is consistent with

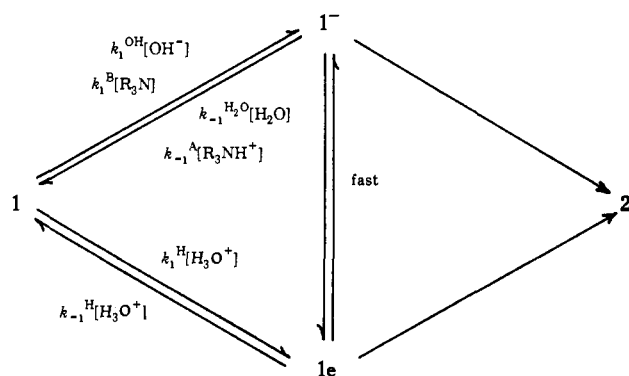
## Scheme V



the observed data if (k<sub>2</sub><sup>H</sup>[H<sub>3</sub>O<sup>+</sup>] + k<sub>2</sub><sup>C</sup>) > k<sub>-1</sub><sup>H</sup>[H<sub>3</sub>O<sup>+</sup>]. Evidence for the rapid hydronium ion catalysis of 1e to 2 has been obtained while studying the reaction of 1 with amines, as described below. It is this catalysis which ensures that enolization is rate determining at all values of [H<sub>3</sub>O<sup>+</sup>].

Scheme VI shows the assignments for all the kinetic

## Scheme VI



terms considered so far (k<sub>B</sub><sup>i</sup>, k<sub>OH</sub><sup>i</sup>, and k<sub>H</sub><sup>i</sup>). In this scheme k<sub>1</sub><sup>OH</sup> is the rate constant for hydroxide ion catalyzed enolate ion formation, and k<sub>1</sub><sup>OH</sup> = k<sub>OH</sub><sup>i</sup> because the initial slope has been assigned to rate-determining α-proton abstraction. Similarly k<sub>1</sub><sup>B</sup> = k<sub>B</sub><sup>i</sup> and k<sub>1</sub><sup>H</sup> = k<sub>H</sub><sup>i</sup>.

In order to be able to deal with absolute values of rate constants in Scheme VI for the reactions of the intermediate enol 1e or enolate anion 1<sup>-</sup>, it is necessary to know the equilibrium concentrations of these species with respect to 1. In the absence of experimental data on the equilibrium concentrations of 1<sup>-</sup> and 1e, it was assumed that the ionization constant and enol content

of 1 are similar to those of cyclohexanone.<sup>29</sup> The measured enol content for cyclohexanone is K<sub>E</sub> = [enol]/[ketone] = 4.1 × 10<sup>-6</sup>, and the ionization constant is K<sub>a</sub><sup>K</sup> = [enolate anion][H<sup>+</sup>]/[ketone] = 10<sup>-16.7</sup>. A pK<sub>a</sub><sup>B</sup> of 11.3 for the enol can be calculated from these data. Using these assumed equilibrium constants, the measured slopes in Table I may be translated into the rate constants listed in Table II.

Microscopic reversibility demands the existence of the k<sub>-1</sub><sup>H<sub>2</sub>O</sup>[H<sub>2</sub>O], k<sub>-1</sub><sup>A</sup>[R<sub>3</sub>NH<sup>+</sup>], and k<sub>-1</sub><sup>H</sup>[H<sub>3</sub>O<sup>+</sup>] terms also shown in Scheme VI. Their values may be calculated from the forward rate constants mentioned above and the assumed equilibria. For example, if k<sub>-1</sub><sup>A</sup>[R<sub>3</sub>NH<sup>+</sup>][1<sup>-</sup>] = k<sub>1</sub><sup>B</sup>[R<sub>3</sub>N][1] at equilibrium, then since K<sub>a</sub> = [R<sub>3</sub>N][H<sub>3</sub>O<sup>+</sup>]/[R<sub>2</sub>NH<sup>+</sup>] and 10<sup>-16.7</sup> = [1<sup>-</sup>][H<sub>3</sub>O<sup>+</sup>]/[1], one can determine that k<sub>-1</sub><sup>A</sup> = k<sub>1</sub><sup>B</sup>K<sub>a</sub>/10<sup>-16.7</sup>. The k<sub>-1</sub><sup>A</sup>, k<sub>-1</sub><sup>H<sub>2</sub>O</sup>, and k<sub>-1</sub><sup>H</sup> constants listed in Table II were all calculated in this manner.

The mechanisms responsible for the conversion of intermediate 1 to 2, manifested in final slope kinetic terms proportional to free amine (k<sub>B</sub><sup>f</sup>), hydroxide ion (k<sub>OH</sub><sup>f</sup>), hydronium ion (k<sub>H</sub><sup>f</sup>), protonated amine (k<sub>A</sub><sup>f</sup>), and a constant (k<sub>C</sub><sup>f</sup>), remain to be considered. It is assumed that 2 can be formed from either 1e or 1<sup>-</sup>, which are in rapid equilibrium. The possibility that either one of these species may be the actual intermediate leads, as we shall see, to certain ambiguities in assignment of mechanisms.

For example, there are several kinetically equivalent plausible postulates for a general base mechanism which would account for the k<sub>B</sub><sup>f</sup>, k<sub>OH</sub><sup>f</sup>, and k<sub>C</sub><sup>f</sup> terms (where the general base in the latter two cases would be hydroxide ion and water, respectively). After elimination of mechanisms with transition states in which only a single proton transfer occurs between two electronegative atoms (and which are therefore unlikely as rate-determining steps<sup>30</sup>), the two mechanisms in Scheme VII appear to be the most reasonable. Scheme VIIa, in which the general base, B, assists in abstraction of the enolic proton, may be criticized because the pK<sub>a</sub> of the enol (11.3) is very close to the pK<sub>a</sub> of the general bases abstracting the proton, and because unstable hydroxide ion is generated. This scheme thus violates the concept<sup>30</sup> that general acid-base catalysis is likely to occur where needed most and in a manner such that unstable (*i.e.*, very high or low pK<sub>a</sub>) species are not produced. Scheme VIIb, on the other hand,

(29) R. P. Bell and P. W. Smith, *J. Chem. Soc. B*, 241 (1966).

(30) Reference 27, Chapter 3.

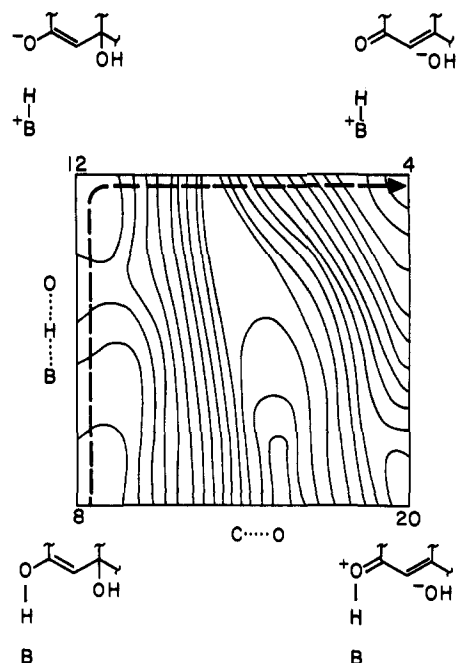


Figure 9. Energy contour diagram for the conversion, according to the mechanism in Scheme VIIa, of enol **1e** to **2** in the presence of a general base **B** with  $pK_a$  of its conjugate acid = 8 and pH 8. Motion of the proton between the enol oxygen and **B** is shown on the vertical axis, and cleavage of the bond between the  $\beta$  carbon and the hydroxyl oxygen is shown on the horizontal axis. The energy levels of the corners of the diagram and of the transition states are in kcal/mol relative to **1** and were calculated as described in the text. The separation between the lines is 2 kcal/mol. The favored pathway will be *via* the enolate anion (upper left-hand corner).

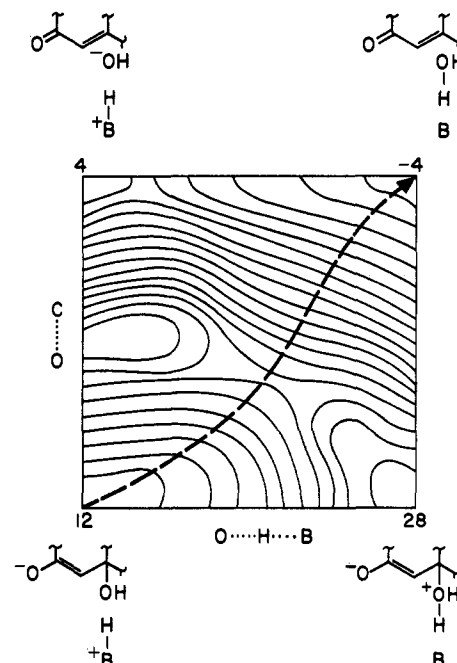
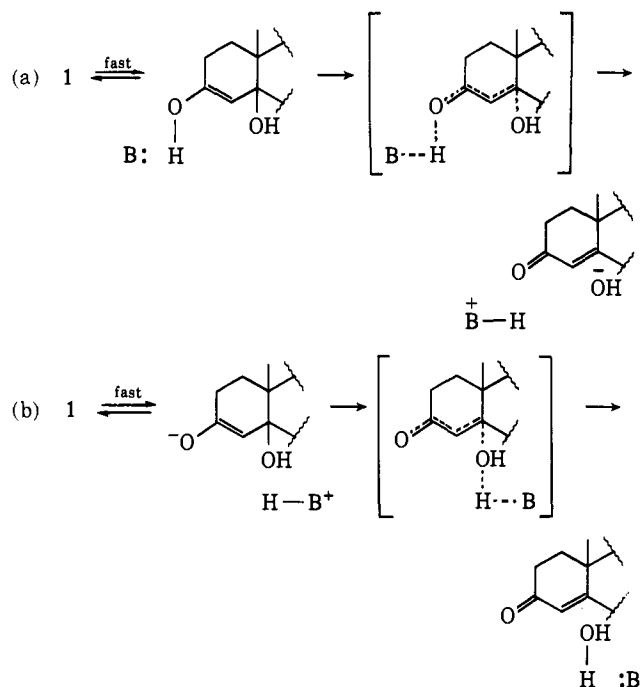


Figure 10. Energy contour diagram for the conversion, according to the mechanism in Scheme VIIb, of enolate anion **1<sup>-</sup>** to **2** in the presence of a general acid **HB** with  $pK_a$  = 8 and pH 8. Motion of the proton between the  $\beta$ -hydroxyl group and **B** is shown on the horizontal axis, and cleavage of the bond between the  $\beta$  carbon and the hydroxyl group is shown on the vertical axis. The energy levels of the corners of the diagram and of the transition states are in kcal/mol relative to **1**, and were calculated as described in the text. The separation between the lines is 2 kcal/mol. The favored pathway will be through the center of the diagram consistent with the observed general acid catalysis with  $\alpha \cong 0.5$ .

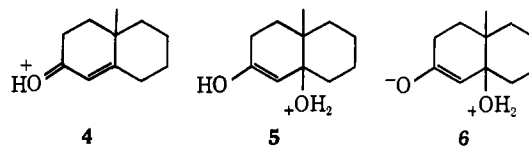
#### Scheme VII



seems more satisfactory because the general acid serves to avoid formation of hydroxide ion.

Energy contour diagrams of the type shown in Figures 9, 10, and 12 have been used by More O'Ferrall<sup>31</sup> and extensively by Jencks<sup>32</sup> to illustrate and systematize

this type of argument. The diagrams in this paper have been constructed in the manner described by Jencks,<sup>32</sup> with energies of intermediates calculated using the assumed equilibrium constants discussed above and assumed  $pK_a$ 's. The  $pK_a$  of **4** was taken to



be  $-4$ , by analogy with known<sup>33</sup> values for protonated enones. Similarly, the  $pK_a$  of **5** was assumed to be  $-2.5$ , in keeping with known values<sup>34</sup> for protonated alcohols. It is difficult to find analogs of **6**, but the inductive effect of the oxy anion should be small through four bonds, and a  $pK_a$  of about  $-1$  seems reasonable. The fact that the conversion of **1** to **2** in aqueous solution goes essentially to completion indicates that  $[2]/[1] \geq 10^3$  at equilibrium and therefore that  $\Delta G \geq -4$  kcal for the overall process. The energy barriers in these diagrams for the conversions  $1^- \rightarrow 2 + \text{OH}^-$ ,  $1e \rightarrow 4 + \text{OH}^-$ ,  $5 \rightarrow 4 + \text{H}_2\text{O}$ , and  $6 \rightarrow 2 + \text{H}_2\text{O}$  were calculated using the expression  $\Delta G^\ddagger = -2.303RT \log(kh/kT)$  from first-order rate constants for these processes obtained from the kinetic data using certain assumptions, as discussed below.

Figure 9 shows the energy surface constructed for Scheme VIIa assuming that the pH is 8 and that  $\text{BH}^+$

(31) R. A. More O'Ferrall, *J. Chem. Soc. B*, 274 (1970).

(32) W. P. Jencks, *Chem. Rev.*, 72, 705 (1972).

(33) G. C. Levy, J. D. Cargioli, and W. Racela, *J. Amer. Chem. Soc.*, 92, 6238 (1970).

(34) N. C. Deno and J. O. Turner, *J. Org. Chem.*, 31, 1969 (1966).

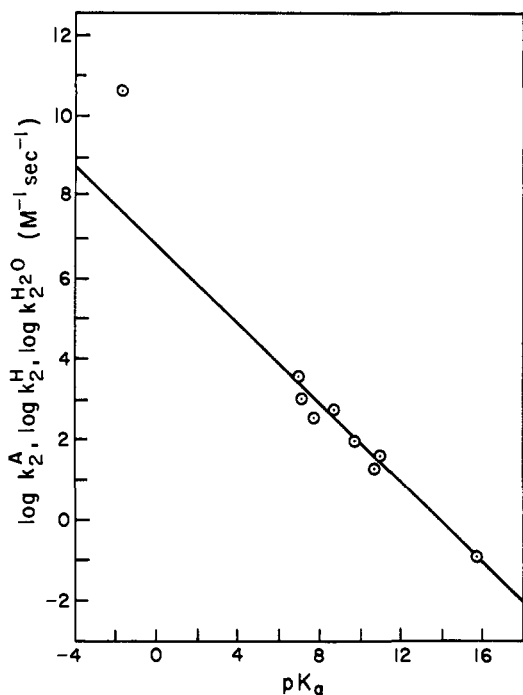


Figure 11. Brønsted plot of log of the second-order rate constants for the reaction of  $1^-$  with general acids ( $k_2^H$ ,  $k_2^A$ ,  $k_2^{H_2O}$ ) vs. the  $pK_a$ 's of the acids. The slope is  $\alpha = -0.5$ .

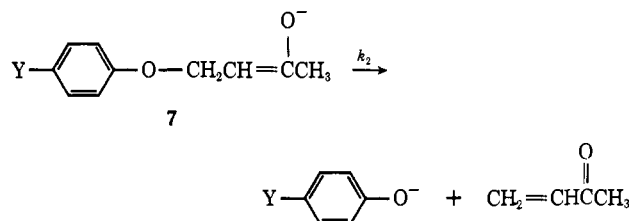
has  $pK_a = 8$ . The proton transfer to form the enolate anion (along the B-H axis in Figure 9) requires little activation energy, whereas formation of **4** and hydroxide ion is estimated below to require about 28 kcal of activation energy. Therefore, the preferred path of reaction should involve formation of intermediate  $1^-$  in the upper left-hand corner. Since proton transfer is complete at the transition state for this mechanism, a Brønsted  $\beta$  of 1.0 would be expected<sup>32</sup> and hydroxide ion should be the only effective catalyst for the reaction. This prediction is inconsistent with the general base catalysis observed and therefore VIIa is not a reasonable mechanism.

A similar surface generated for Scheme VIIb, shown in Figure 10, is more consistent with the observed catalysis by general bases. Because the expulsion of hydroxide ion from  $1^-$  involves the considerable activation energy necessary to break the O-C bond, a diagonal route will be of lowest energy, consistent with general acid catalysis. The energy barrier of 16 kcal indicated in Figure 10 for the uncatalyzed decomposition of  $1^-$  to **2** plus hydroxide ion was calculated from the value of  $k_2^C$ , determined as discussed below.

The final slopes proportional to general base concentration ( $k_B^f$ ) are therefore proposed to reflect the specific base-general acid mechanism shown in Scheme VIIb. Using this scheme and the previously assumed equilibrium constants, the rate constants  $k_2^A$  for general acid catalysis of the reaction of  $1^-$  to **2** can be computed from the values of  $k_B^f$  listed in Table I. Since  $k_2^A \cdot [R_3NH^+][1^-] = k_B^f[R_3N][1]$ , then  $k_2^A = k_B^f K_a / 10^{-16.7}$ , where  $K_a$  is the dissociation constant for the protonated amine. The values of  $k_2^A$  thus computed are listed in Table II and their logarithms are plotted vs. amine  $pK_a$  to afford the Brønsted plot for the conversion of  $1^-$  to **2** shown in Figure 11. A Brønsted  $\alpha$  of 0.5 is obtained for this catalysis by ammonium ions.

Also included in Figure 11 are points calculated from the values of  $k_C^f$  and  $k_{OH}^f$  by assuming that  $BH^+$  in Scheme VIIb is hydronium ion and water, respectively. Such "end points" are often troublesome because the hydroxide ion or hydronium ion used or generated in such catalysis may be of sufficiently high energy to distort the energy surface markedly from the pattern established by weaker acids and bases. The point in Figure 11 at  $pK_a = 15.7$  represents the second-order rate constant,  $k_2^{H_2O}$ , which was calculated from  $k_{OH}^f$  by assuming that water catalyzes the loss of hydroxide ion from  $1^-$ , just as protonated amines do, using 55 M as the water concentration. However, if Figure 10 were reconstructed for the case where  $BH^+$  is water ( $pK_a = 15.7$ ) and B is hydroxide ion, the upper-left and upper-right corners of the energy contour would be equivalent, with a negligible energy barrier between them. The second-order reaction of  $1^-$  with water to form **2**,  $OH^-$ , and  $H_2O$  would be energetically equivalent to the first-order decomposition of  $1^-$  to form **2** and  $OH^-$ , and it would be pointless to postulate general acid catalysis by water.<sup>35</sup> The first-order rate constant for the unimolecular decomposition of  $1^-$  to **2**,  $k_2^C$ , is therefore simply the  $k_2^{H_2O}$  value on the Brønsted line  $\times 55 M = 7.83 \times 10^1 \text{ sec}^{-1}$ . This value of  $k_2^C$  was important in the construction of Figure 10, as noted above.

The other "end point" in Figure 11 at  $pK_a = -1.7$  can be assigned as the rate constant for hydronium ion catalysis of  $1^-$  to **2**, calculated from  $k_C^f$ . This point deviates by two positive logarithmic units from the line drawn through the protonated amine and water points, and has an absolute value,  $4.05 \times 10^{10} \text{ M}^{-1} \text{ sec}^{-1}$ , which is roughly equal to the diffusion-controlled limit for reactions in aqueous solution.<sup>36</sup> This suggests that the reaction of  $1^-$  with hydronium ion follows a substantially different path from that of  $1^-$  with protonated amines. Since the  $pK_a$  of **6** is probably slightly higher than that of hydronium ion, the proton transfer in the first step is probably slightly exothermic and occurs at a diffusion-controlled rate.<sup>36</sup> If the intermediate **6** has no appreciable lifetime and breaks down to product with a rate greater than  $k_{-1}$ , then assignment of the  $k_C^f$  as rate-determining formation of **6** is reasonable. Evidence that  $k_2$  is indeed very large can be obtained by extrapolation of Fedor's data<sup>6</sup> for the rate constants ( $k_2$ ) for unimolecular decomposition of a series of enolate anions (**7**). A plot of  $\log k_2$  vs.  $pK_a$  of



the corresponding phenol forms a slope yielding  $k_2 = 10^{11} \text{ sec}^{-1}$  for a  $pK_a$  of  $-1.7$ . The energy barrier in Figure 10 for the conversion of **6** to **2** is shown as  $\approx 2$  kcal/mol, consistent with a  $k_C^f$  term which reflects rate-

(35) W. P. Jencks, *J. Amer. Chem. Soc.*, **94**, 4731 (1972), formulates this type of argument as a rule for the reverse reaction, stating that hydroxide ion will not act as a general base catalyst for the nucleophilic addition of water.

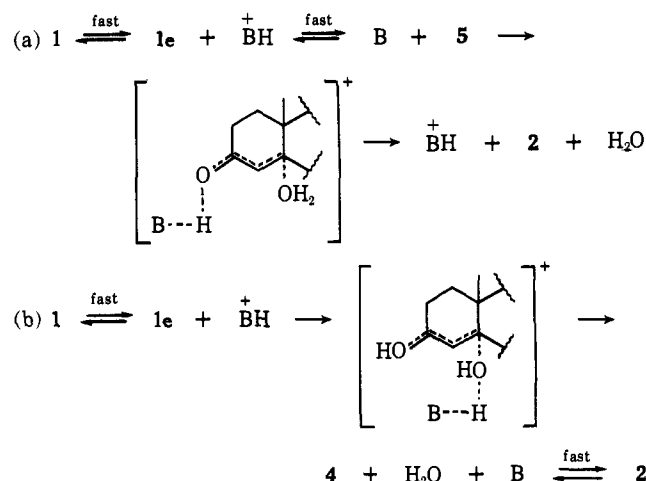
(36) Reference 27, pp 207-211.

determining, diffusion-controlled proton transfer from  $\text{H}_3\text{O}^+$  to  $1^-$  to form **6**. Such an interpretation seems much more consistent with the rest of this study than does postulation of the kinetically equivalent rate-determining water catalyzed decomposition of **1e**.

The fact that the  $\beta$ -phenoxy enolate anions **7** do not show general acid catalysis for the formation of enone<sup>6</sup> is also consistent with Scheme VIIb, but not VIIa. The energy map in Figure 10 for mechanism VIIb is altered when the leaving group is phenoxide rather than hydroxide ion so as to favor passage through the upper left-hand corner. Since  $\alpha = 0$  for this path, catalysis of the breakdown of enolate anion would not be expected to be observable.

The final slopes  $k_A^f$  and  $k_H^f$ , proportional to protonated amine and hydronium ion, respectively, represent general acid catalysis of the conversion of intermediate to product. Two possible, kinetically equivalent, mechanisms for these terms are shown in Scheme VIII. Scheme VIIIa postulates general-base abstrac-

#### Scheme VIII



tion of the enolic proton from **5**. As in the analogous mechanism VIIa above, there is presumably little need for general base catalysis of the removal of this proton and accordingly this pathway is considered to be unlikely.

Scheme VIIIb, involving general acid catalysis of removal of hydroxide ion from **1e**, is shown in Figure 12. Substantial energy barriers exist for either of the stepwise processes involving  $1e \rightarrow 4$  or  $1e \rightarrow 5$ . A more favorable path is available through the center of the energy diagram, consistent with the rough value of  $\alpha \approx 0.7$  for general acid catalysis obtained from a line drawn through values of  $\log k_H^f$  and  $\log k_A^f$  plotted vs.  $\text{p}K_a$ 's. The mechanism shown in Scheme VIIIb accordingly is assigned to these observed  $k_A^f$  and  $k_H^f$  terms, with  $\text{BH}^+$  being protonated amine and hydronium ion, respectively. The rate constants in Table II for the reaction of **1e** with protonated amine ( $k_3^A$ ) or hydronium ion ( $k_3^H$ ) were calculated using the assumed enol content<sup>29</sup> and the observed values of  $k_A^f$  and  $k_H^f$ .

The energy barrier of  $\sim 6$  kcal/mol shown in Figure 12 for the conversion of **5** to **4** plus water was obtained from  $k_3^H$  and the  $\text{p}K_a$  of **5**, by assuming that  $k_{5 \rightarrow 4}[\text{5}] = k_3^H[\text{H}_3\text{O}^+][1e]$ . The energy barrier of  $\sim 28$  kcal in Figures 9 and 12 for the conversion of **1e** to **4** plus hydroxide ion was obtained by extrapolation of  $\log k_3^H$

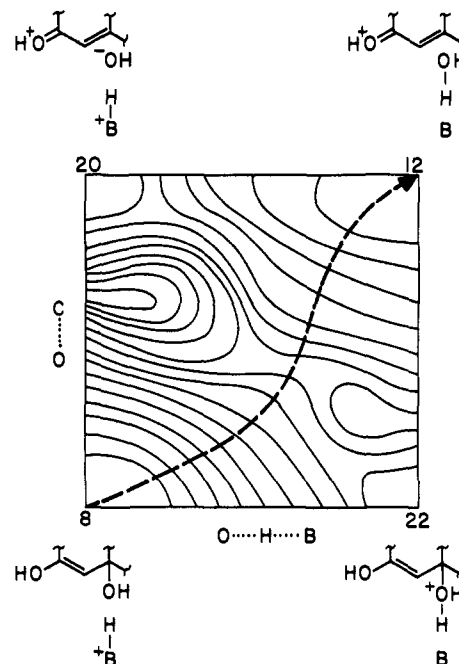
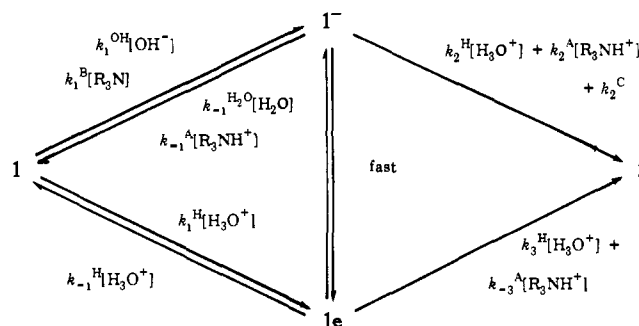


Figure 12. Energy contour diagram for the conversion, according to the mechanism in Scheme VIIIb, of enol **1e** to **2** in the presence of a general acid  $\text{HB}^+$  with  $\text{p}K_a = 8$  at pH 8. Motion of the proton between  $\text{BH}^+$  and the hydroxyl group is shown on the horizontal axis, and cleavage of the bond between the  $\beta$  carbon and the hydroxyl oxygen is shown on the vertical axis. The energy levels of the corners of the diagram and of the transition states are in kcal/mol relative to **1** and were calculated as described in the text. The separation between the lines is 2 kcal/mol. The favored pathway will be through the center of the diagram consistent with the observed general acid catalysis with  $\alpha \cong 0.7$ .

and  $\log k_3^A$  values to a  $\text{p}K_a$  of 15.7, followed by division of the second-order rate constant thus obtained by  $[\text{H}_2\text{O}] = 55 M$  (analogously to the determination of  $k_2^C$  from  $k_2^{\text{H}_2\text{O}}$ ) to give the desired first-order rate constant.

All of the observed slopes in Table I have now been assigned to specific mechanisms and the rate constants involved in those mechanisms have been computed and listed in Table II. Scheme IX summarizes the entire

#### Scheme IX



mechanistic scheme for the dehydration of **1** to form **2**.

The evidence for general acid-base catalysis of the breakdown of intermediate to product amply observed in this investigation had been found in none of the previous studies of carbanionic elimination reactions,<sup>37</sup> including those involving relatively poor leaving

(37) T. I. Crowell and A. W. Francis, Jr., *J. Amer. Chem. Soc.*, **83**, 591 (1961), have observed general base-catalyzed addition of water to nitrostyrenes to give stabilized carbanions, in an example of the reverse reaction.

groups.<sup>5,7,8,10,11</sup> In all<sup>7,8,10,11</sup> but one of those studies, no attempt was made to study changes in rate with varying buffer concentrations, so that such catalysis could not have been detected. However, in Fedor's study<sup>5</sup> of the loss of methanol from  $\beta$ -methoxy ketones, the rate depended only on hydroxide ion concentration and not on the concentration of amine buffers. We have no explanation for the discrepancy between Fedor's observations and those presented here. Our observations of the importance of general base catalysis for the formation of carbanionic intermediate and of general acid catalysis of expulsion of hydroxide ion from that intermediate are consistent with the mechanism proposed for the action of  $\beta$ -hydroxydecanoyl thioester dehydrase.<sup>16,18</sup>

### Experimental Section

**Materials.** 9-Hydroxy-10-methyl-*cis*-decalone-2 (**1**) was prepared by the method of Marshall and Fanta.<sup>25</sup> 1,1,3,3,8,8-Hexadeuterio-9-hydroxy-10-methyl-*cis*-decalone-2 (**1-C<sub>1</sub>-d<sub>6</sub>**) was prepared by oxidation of 1,1,2,3,3,8,8-heptadeuterio-2,9-dihydroxy-10-methyl-*cis*-decalin, which was obtained as previously described.<sup>1</sup> To a solution of 0.62 g (3.35 mmol) of this labeled diol in 30 ml of reagent grade acetone was added 1.0 ml (8.0 mmol) of 8 *N* Jones reagent<sup>26</sup> at room temperature. After 15 min the reaction mixture was poured into 150 ml of a 5% aqueous KHCO<sub>3</sub> solution, which was then extracted with four 30-ml portions of ether. The extracts were combined, washed with 20 ml of saturated aqueous NaCl solution, dried over MgSO<sub>4</sub>, and evaporated to yield a solid residue which afforded, after recrystallization from 1:1 ether-hexane, 0.40 g (66%) of **1-C<sub>1</sub>-d<sub>6</sub>**, mp 119–120°; ir (KBr) 2.94, 4.5–4.8, and 5.86  $\mu$ .

Liquid amines used as catalysts were purified either by two recrystallizations of the hydrochloride from 1:1 methanol-1-propanol, or by distillation twice from barium oxide directly before use. The solid amines, imidazole and 1,4-diazabicyclo[2.2.2]octane, were purified by recrystallization twice from ether.

**Apparatus.** A Unicam SP 800B spectrophotometer equipped with an automatic cell changer and timed by a Cary 1116100 program timer was used to obtain data on four runs simultaneously. The temperature within the cuvettes was maintained at 25.0  $\pm$  0.1° by circulating water with temperature controlled by a P. V. Tamson bath through the cuvette housing. A Cary 14 spectrophotometer, similarly equipped, was used for ultraviolet wavelength scans and for the experiments involving the very slow reaction of **1** at pH's near neutrality, which necessitated special procedures. A 10-cm silica cell was constructed so that a magnetic stirring bar could be placed in its bottom and a pH meter electrode fitted into its top, within the cell compartment of the Cary 14. This arrangement allowed both stirring of the reaction mixture and constant monitoring of the pH during the reaction, while the cell remained sealed to prevent CO<sub>2</sub> absorption. Measurements of pH were made with a Radiometer

Model 26 pH meter equipped with a GK2302C combination electrode.

**Kinetics.** The methods used to obtain  $k_{\text{obsd}}$  values for the formation of **2** from **1** were identical with those previously described<sup>1</sup> for the conversion of keto acetate **3** to **2**, except as follows. For a series of  $k_{\text{obsd}}$  values obtained by varying amine concentration at constant pH, it was desirable to correct for small differences in  $k_{\text{obsd}}$  values caused by unavoidable minor variations in pH. This was accomplished by correcting all  $k_{\text{obsd}}$  values obtained in such a series by choosing a hydroxide ion concentration,  $[\text{OH}^-]_{\text{cor}}$ , and using the expression

$$k_{\text{obsd cor}} = k_{\text{obsd uncor}} - (f_{\text{OH}}[\text{OH}^-]_{\text{obsd}} - f_{\text{OH}}[\text{OH}^-]_{\text{cor}})$$

The value of  $f_{\text{OH}}[\text{OH}^-]$  was computed from eq 3, using the rate constants in Table I. The values of  $k_{\text{obsd}}$  in this paper which are part of a series at a specified pH are all  $k_{\text{obsd cor}}$  values.

The rates of dehydration of **1** in unbuffered aqueous solution near neutrality were obtained using relatively concentrated solutions of **1** ( $\sim 3 \times 10^{-3}$  *M*) in doubly distilled water which had been boiled just prior to use. The solution within the 10-cm cell described above was stirred magnetically, and the pH of the solution was continually monitored with the pH meter electrode inserted in the solution. A seal was obtained between the electrode and the neck of the cell by use of a neoprene ring and Parafilm. The desired pH for each run was obtained by the appropriate addition of several drops of dilute NaOH solution, followed by sealing of the system, and measurement of pH after waiting 1 hr for the hydration of any CO<sub>2</sub> present. The absorbance reading at 247 nm was then taken at intervals of 30–60 min, and  $k_{\text{obsd}}$  was computed using the first reading as  $A_0$ . The pH control was excellent and drifts of less than 0.1 pH unit were obtained in each case after the initial stabilization period. Since the  $A_{247}$  at these concentrations of **1** is high ( $A_{247} \sim 500$ ), less than 0.1% of the reaction was observed. The substantial absorbance of ketol **1** at these concentrations was assumed to be constant throughout the run.

**Acknowledgment.** Funds which enabled purchase of the Unicam spectrophotometer used in this research were provided by PHS Grant AM 11815 from the National Institute for Arthritis and Metabolic Diseases and general support was provided by National Science Foundation Grant No. GP-34390X. The authors are also grateful for the support provided to D. J. H. by an NSF Traineeship (1968–1971) and a Goodyear Foundation Fellowship (1971–1972), and to G. T. S. by a NASA Traineeship. Professor R. L. Cleland generously loaned us a constant temperature water circulator. Several coworkers, particularly Dr. Eberhard Kiehlmann, obtained preliminary data on the conversion of **1** to **2** under very frustrating experimental circumstances. We are also greatly indebted to Professor Maynard V. Olson for extensive assistance in the derivation of kinetic expressions and to Professor William P. Jencks for extremely helpful discussions and for a preprint of ref 32.

(38) A. Bowers, T. G. Halsall, E. R. H. Jones, and A. J. Lemin, *J. Chem. Soc.*, 2548 (1953).